Characterization of the Membrane Domain Subunit NuoK (ND4L) of the NADH−Quinone Oxidoreductase from Escherichia coli † , ‡

ARTICLE *in* BIOCHEMISTRY · AUGUST 2005

Impact Factor: 3.02 · DOI: 10.1021/bi050708w · Source: PubMed

4 AUTHORS, INCLUDING:

Mou-Chieh Kao
National Tsing Hua University
17 PUBLICATIONS **427** CITATIONS

SEE PROFILE

Eiko Nakamaru-Ogiso
University of Pennsylvania
65 PUBLICATIONS **1,498** CITATIONS

SEE PROFILE

Characterization of the Membrane Domain Subunit NuoK (ND4L) of the NADH-Quinone Oxidoreductase from *Escherichia coli*[†,‡]

Mou-Chieh Kao, Eiko Nakamaru-Ogiso, Akemi Matsuno-Yagi,* and Takao Yagi*

Division of Biochemistry, Department of Molecular and Experimental Medicine, The Scripps Research Institute, 10550 North Torrey Pines Road, La Jolla, California 92037

Received April 18, 2005; Revised Manuscript Received May 12, 2005

ABSTRACT: The ND4L subunit is the smallest mitochondrial DNA-encoded subunit of the proton-translocating NADH-quinone oxidoreductase (complex I). In an attempt to study the functional and structural roles of the NuoK subunit (the *Escherichia coli* homologue of ND4L) of the bacterial NADH-quinone oxidoreductase (NDH-1), we have performed a series of site-specific mutations on the *nuoK* gene of the NDH-1 operon by using the homologous recombination technique. The amino acid residues we targeted included two highly conserved glutamic acids that are presumably located in the middle of the membrane and several arginine residues that are predicted to be on the cytosolic side. All point mutants examined had fully assembled NDH-1 as detected by blue-native gel electrophoresis and immunostaining. Mutations of nearly perfectly conserved Glu-36 lead to almost null activities of coupled electron transfer with a concomitant loss of generation of electrochemical gradient. A significant diminution of the coupled activities was also observed with mutations of another highly conserved residue, Glu-72. These results may suggest that both membrane-embedded acidic residues are important for the coupling mechanism of NDH-1. Furthermore, a severe impairment of the coupled activities occurred when two vicinal arginine residues on a cytosolic loop were simultaneously mutated. Possible roles of these arginine residues and other conserved residues in the NuoK subunit for NDH-1 function were discussed.

The mitochondrial respiratory chain is composed of five enzyme complexes. Among them, the NADH-quinone oxidoreductase (complex I[1]) is the largest, most intricate, and least understood (*1*). Complex I catalyzes the first step of electron transport by the oxidation of NADH thus providing two electrons for the reduction of quinone to quinol. This electron-transfer process in the complex I is coupled to the translocation of four protons across the inner membrane to generate an electrochemical proton gradient (*2*). Forty-six different subunits have been identified in complex I from bovine heart mitochondria with a combined molecular mass of almost 1000 kDa (*3*). In contrast to the mitochondrial enzyme, the bacterial H^+-translocating NADH-quinone oxidoreductase (NDH-1) contains only 13 or 14 subunits (designated Nqo1−14 for *Paracoccus denitrificans* and *Thermus thermophilus* and NuoA-N for *Escherichia coli*)[2] (*4*, *5*). All bacterial subunits are homologues of the subunits of the mitochondrial core enzyme and represent the minimal requirement for sufficient energy transduction by complex I (*6*).

Because of its complexity, unlike other respiratory chain complexes, an X-ray structure of complex I is not available at this moment. Low-resolution images obtained from electron microscopy analyses indicated that the bacterial NDH-1 has two arms arranged perpendicular to each other that form a characteristic L-shaped structure (*7*). The peripheral arm protrudes into the cytoplasm, and the membrane arm is embedded within the cytoplasmic membrane. The peripheral arm is made up of seven subunits (NuoB, -C, -D, -E, -F, -G, and -I) which are homologous to seven nuclear-encoded subunits in mitochondrial complex I. In *E. coli*, the NuoC (30 kDa) and NuoD (49 kDa) subunits form a single subunit (NuoCD) (*8*). This domain harbors one noncovalently bound FMN and 8−9 iron−sulfur clusters and carries the binding site for NADH (*9*, *10*). Two of the peripheral subunits, NuoB (PSST) and NuoI (TYKY), have

[†] This work was supported by U.S. Public Health Service Grants R01GM33712 (to A.M.-Y. and T.Y.). Synthesis of oligonucleotides and DNA sequencing were, in part, supported by the Sam & Rose Stein Endowment Fund.

[‡] This is publication 17309-MEM from The Scripps Research Institute, La Jolla, CA.

* To whom correspondence should be addressed: Takao Yagi or Akemi Matsuno-Yagi, Division of Biochemistry, Department of Molecular and Experimental Medicine, The Scripps Research Institute, 10550 North Torrey Pines Road, La Jolla, CA 92037. Phones, 858-784-8094 or 858-784-2596; fax, 858-784-2054, e-mails, yagi@scripps.edu (for T.Y.) or ayagi@scripps.edu (for A.M.-Y.).

[1] Abbreviations: NDH-1, bacterial H^+-translocating NADH-quinone oxidoreductase; complex I, mitochondrial H^+-translocating NADH-quinone oxidoreductase; NDH-2, bacterial NADH-quinone oxidoreductase lacking the energy coupling site; DB, dimethoxy-5-methyl-6-decyl-1,4-benzoquinone; dNADH, reduced nicotinamide hypoxanthine dinucleotide (deamino-NADH); Spc, spectinomycin; PCR, polymerase chain reaction; BN-PAGE, blue-native polyacrylamide gel electrophoresis; EDTA, ethylenediaminetetraacetic acid; PMSF, phenylmethanesulfonyl fluoride; DTT, dithiothreitol; Q, quinone(s); cap-40, capsaicin-40; Bistris, 2-[bis(2-hydroxyethyl)amino]-2-(hydroxymethyl)-propane-1,3-diol; MOPS, 3-(*N*-morpholino)propane-sulfonic acid; oxonol VI, bis-(3-propyl-5-oxoisoxazol-4-yl)pentamethine oxonol; ACMA, 9-amino-6-chloro-2-methoxyacridine; FCCP, carbonyl cyanide *p*-trifluoromethoxyphenylhydrazone; TM, transmembrane.

[2] For simplicity, the *E. coli* terminology was mainly used throughout this paper. Bovine naming was also used as needed for clarity.

10.1021/bi050708w CCC: $30.25
Published on Web 06/16/2005

the connector function bridging the peripheral and the membrane arms (*11*−*13*). The membrane arm also consists of seven subunits (NuoA, -H, -J, -K, -L, -M, and -N) (*14*−*16*), which are homologues of mtDNA-encoded subunits (ND1−6 and ND4L) (*17*, 18). Unlike the peripheral arm, the membrane arm does not contain any identified redox prosthetic groups. Despite recent progress in the development of tools for structural biology studies, information about the functional and structural roles of these membrane-bound subunits is still limited. Nevertheless, it is most likely that these membrane-bound subunits are involved in H^+ translocation and quinone and inhibitor binding (*19*−*21*).

Subunit NuoK (mitochondrial ND4L subunit) is the smallest of the membrane domain subunits of the NDH-1. There have been several observations that may indicate involvement of the NuoK subunit in the essential function of the NDH-1. For example, disruption of the *nuoK* gene in *Rhodobacter capsulatus* leads to the inactivation of NDH-1 activity (*22*). Also, it has been pointed out that NuoK/ND4L is evolutionally related to the membrane-bound type-4 hydrogenase, HyfE, of *E. coli* (*23*) and to one particular class of antiporters, MrpC (*24*). It was further suggested that a multisubunit antiporter module of MrpC containing the NuoKLMN homologues was recruited to the ancestral complex I and might play a role in the proton translocation machinery. Previously, we experimentally determined the topology of the *Paracoccus* NuoK subunit (*15*). The *Paracoccus* NuoK subunit is composed of three transmembrane segments (named TM1−3 from the N- to the C-terminus) with the N- and C-terminal region facing the periplasmic and cytoplasmic side of the membrane, respectively. According to the proposed topology of the NuoK subunit, there are two highly conserved glutamic acid residues located in the middle of the transmembrane spans (TM2 and TM3). It was, therefore, speculated that these two residues might play important roles in the coupling mechanism of NDH-1/complex I. In fact, Kervinen et al. (*25*) recently reported that mutating or moving the two glutamates of the *E. coli* NDH-1 could severely impair the electron transfer activity and cell growth. To further study the roles of the two glutamic acids as well as other charged residues in this subunit, we chose to introduce mutations directly in the *E. coli* chromosomal NDH-1 operon to mimic the real situation in the living cells. Using this approach, we constructed a series of mutants and characterized them with regard to coupled activities and assembly of the NDH-1. The results indicated that the NuoK subunit is required for proper *E. coli* NDH-1 function.

EXPERIMENTAL PROCEDURES

Materials. DCCD, dNADH, DB, chloramphenicol, and spectinomycin (Spc) were from Sigma (St. Louis, MO). Capsaicin 40 (cap-40) was kindly provided by Dr. Hideto Miyoshi (Kyoto University, Kyoto, Japan). Bis-(3-propyl-5-oxoisoxazol-4-yl)pentamethine oxonol (oxonol VI) and 9-amino-6-chloro-2-methoxyacridine (ACMA) were purchased from Molecular Probes (Eugene, OR). The pCRScript Cloning kit was from Stratagene (La Jolla, CA). Site-directed mutations were generated by using the GeneEditor Mutagenesis Kit from Promega (Madison, WI). The gene replacement vector, pKO3, was a generous gift from Dr. George M. Church (Harvard Medical School, Boston, MA). Materials for plasmid preparation, PCR product purification, and gel extraction were obtained from Qiagen (Valencia, CA). The BCA protein assay kit, SuperSignal West Pico chemiluminescent substrate, and Imject Activated Immunogen Conjugation kit were obtained from Pierce (Rockford, IL).

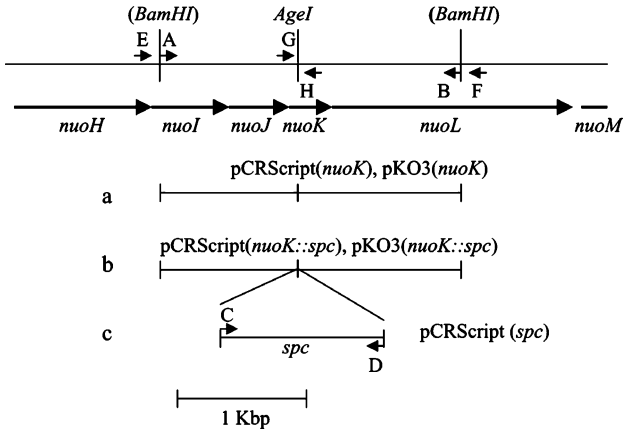

FIGURE 1: Schematic representation of the strategy of *nuoK* cloning, insertion of a Spc cassette in the *E. coli nuoK* gene, and construction of site-specific *nuoK* mutants. Arrows (A−H) illustrate the primers used in this study. The restriction enzymes in the parentheses are newly introduced into the *E. coli* DNA.

Cloning and Mutagenesis of the E. coli nuoK Gene. The strategies used for cloning and mutagenesis of the *E. coli nuoK* gene were in principle similar to those we reported for the *nuoJ* gene (*26*) and illustrated in Figure 1. A DNA fragment, which includes the *nuoK* gene, its upstream 1-kb DNA segment, and its downstream 1-kb DNA segment, was amplified from *E. coli* DH5α by PCR using primer A (5′-*GGATCC*GTTATCGTGGTCGTATCGTTC-3′) and primer B (5′-*GGATCC*TCAAGTGGAAAATCGCCGCATC-3′). The italicized bases represented the introduced restriction site *Bam*HI on both ends of the cloned fragment, and the underlined bases were altered from *E. coli* DNA. The spectinomycin-encoding gene from transposon Tn554 of *Staphylococcus aureus* (*27*) was obtained by PCR amplification using the sense primer C (5′-*ACCGGT*CAGTGGAACGAAAACTCACGTTAAG-3′) and the antisense primer D (5′-*ACCGGT*TTCTTTCTATTTTCAATAGTTAC-3′) both containing an *Age*I restriction site (italicized). The amplified DNA fragments containing the *nuoK* gene and the Spc cassette were then individually subcloned into pPCR-Script Amp SK(+) by following the manufacturer's protocol, and their sequences were verified by sequencing. The resulting plasmids were designated pCRScript(*nuoK*) and pCRScript-(*spc*), respectively (Figure 1a,c).

Introduction of a site-specific mutation directly into the *nuoK* gene of the *E. coli* NDH-1 operon requires the generation of a *nuoK* gene knock-out mutant. We employed a chromosomal mutagenesis system based on homologous recombination specifically designed for *E. coli* (*28*). In this gene replacement system, the pKO3 vector used contains a temperature-sensitive replication origin, *repA*(Ts), a chloramphenicol-resistant gene (*cat*), and a *Bacillus subtilis sacB* gene encoding levansucrase. These characteristics make possible the positive and negative selection for chromosomal integration and excision. The construction of the pKO3 carrying NuoK knock-out DNA was shown in Figure 1b. Because the *E. coli nuoK* gene has a naturally occurring *Age*I site which is located close to the 5′ end of the gene, an *Age*I−

Table 1: Primers for Introduction of a Site-Specific Mutation into the *E. coli* NuoK Subunit

mutation	mutagenic primer sequence[a]
R25A	5′-GGTCTGGTTATCGCTCGCAATCTGCTGTTTATG-3′
R25K	5′-GGTCTGGTTATCAAGCGCAATCTGCTGTTTATG-3′
E36A	5′-GTTGATTGGTCTGGCAATCATGATTAACG-3′
E36Q	5′-GTTGATTGGTCTGCAAATCATGATTAACG-3′
E72A	5′-GCGGCGGCAGCAGCGAGTATC-3′
E72Q	5′-GCGGCGGCACAAGCGAGTATC-3′
R85A	5′-TGCAACTTCACGCTCGTCGCCAGAAC-3′
R85K	5′-CTGCAACTTCACAAACGTCGCCAGAACCTG-3′
R87A	5′-ACTTCACCGTCGTGCCCAGAACCTGAAC-3′
R87K	5′-AACTTCACCGTCGTAAACAGAACCTGAACATC-3′
F15A	5′-CTCGCGGCAATCTTAGCCGTTCTTGGCTTAACCG-3′
G21V	5′-CGTTCTTGGCTTAACCGTTCTGGTTATCCGTCGC-3′
R26A	5′-CCGGTCTGGTTATCCGTGCCAATCTGCTGTTTATGTTG-3′
R26K	5′-TAACCGGTCTGGTTATCCGTAAGAATCTGCTGTTTATGTTGATTGGTC-3′
R25A/R26A	5′-CCGGTCTGGTTATCGCTGCCAATCTGCTGTTTATGTTG-3′

[a] Underline indicates mutation.

*Age*I fragment carrying a Spc cassette can be directly inserted into the *E. coli nuoK* gene without making alterations to its original sequence. Therefore, the pCRScript(*spc*) was digested with *Age*I, and the DNA fragment containing the Spc cassette was then purified and ligated into the *Age*I-digested pCRScript(*nuoK*) to generate a plasmid named pCRScript (*nuoK*::*spc*). A *Bam*HI−*Bam*HI fragment digested from this construct was then cloned into the *Bam*HI site of pKO3 to produce pKO3(*nuoK*::*spc*).

To prepare the pKO3 vectors carrying mutated *nuoK* genes, the pCRScript(*nuoK*) was first mutagenized individually with the synthetic oligonucleotides listed in Table 1 using the GeneEditor in vitro site-directed mutagenesis system (Promega) according to the manufacturer's instructions to introduce the *nuoK* point mutations. The generation of desired mutations was confirmed by DNA sequencing using primer G (5′-CTTACAACATGGACTGATCCTCG-3′) and/or primer H (5′-TCACTTACTGAATCGATGTTCAGG-3′). As seen in Figure 1, these two primers are situated within the *nuoK* gene and located upstream and downstream of the intended mutation sites, respectively. The above pCRScript constructs were then digested with *Bam*HI, and DNA fragments containing the desired *nuoK* point mutations were finally transferred to integration plasmid pKO3 at the *Bam*HI site. The resulting plasmids were referred to as pKO3(*nuoK* mutants). To evaluate possible effects of the entire process of gene manipulation in generation of point mutations on the *E. coli* cells, we also constructed a control pKO3 vector, designated pKO3(*nuoK*), using the same procedure except that the wild-type *nuoK* gene derived from pCRScript(*nuoK*) without any mutation was inserted into the *Bam*HI site of pKO3.

Preparation of Knock-Out and Mutant Cells. The pKO3-(*nuoK*::*spc*) gene replacement vector which carried the NuoK knock-out allele was transformed into *E. coli* strain MC4100 (*F*$^-$*, araD139,* Δ*(arg F-lac)U169, ptsF25, relA1, flb5301, rpsL 150.λ*$^-$). The occurrence of homologous recombination, which depended on chromosomal integration and excision, was evaluated using the selection procedure developed by Link et al. (*28*) with some minor modifications as described previously (*29*). After selection of the plausible clones, colony PCR was performed with primer E (5′-ACGCGAATGTACCCGGAAGAGC-3′) and primer D or with primer C and primer F (5′-AGATGTTCTGTTCGTGATGGCAG-3′). Primer C and primer D were located within the Spc cassette, and the primer E and primer F were complementary to upstream and downstream of the cloned *E. coli* chromosome, respectively. By checking the size of the amplified DNA fragment, not only the presence of the Spc cassette but also its location in the genomic DNA could be confirmed. The NuoK knock-out MC4100 cells were first grown in 2× YT medium and then made competent. Later, these competent cells were applied to introduce *nuoK* point mutations in the *E. coli* genome using a similar procedure as just described except that the selection of the candidate recombinants was carried out by screening for spectinomycin sensitivity in addition to chloramphenicol sensitivity. The control mutant (KO-rev) was generated in the same way except that, instead of using pKO3(*nuoK* mutants), the pKO3(*nuoK*) carrying the wild-type *nuoK* gene was employed in the recombination process. Following the selection process, possible colonies were subjected to colony PCR with the sense primer E and the antisense primer H to amplify *nuoK*-containing DNA fragments. The correct introduction of point mutations in the chromosome was finally confirmed by direct sequencing of these amplified fragments using primer G. Bacterial cell culture and membrane preparation were carried out as reported earlier (*26*).

Antibody Production. To facilitate the identification of the NuoK subunit, an oligopeptide, H-CLNIDSVSEMRG-OH (designated NuoKc), derived from the C-terminal region of the *E. coli* NuoK subunit with an extra cysteine incorporated for conjugation, was linked to maleimide-activated bovine serum albumin (Pierce, Rockford, IL) to serve as an immunogen according to the manufacturer's instructions. Antibodies against the C-terminal regions of *E. coli* NuoA and NuoJ subunits had previously been produced in a similar way (*26*, *29*). In contrast, the inclusion bodies of overexpressed NuoB, NuoCD, NuoE, NuoF, NuoG, and NuoI subunits were used for raising these peripheral subunit-specific antibodies in rabbits (*9*). The antibodies were affinity-purified according to Han et al. (*30*).

Gel Electrophoresis and Immunoblotting Analysis. Ten micrograms of protein samples from each membrane suspension was first subjected to SDS−PAGE according to Laemmli (*31*), followed by transferring to nitrocellulose membranes and identification of individual subunits using affinity-purified, subunit-specific antibodies. The assembly of NDH-1

was evaluated by using BN-PAGE according to Schägger and von Jagow (*32*) with some minor modifications. Briefly, the *E. coli* membrane samples containing 800 μg of protein were resuspended in 40 μL of 50 mM Bistris-HCl (pH 7.0) buffer with 750 mM aminocaproic acid, followed by membrane solubilization through the addition of 6 μL of 10% (w/v) *n*-dodecyl-β-maltoside and 50 μg/mL DNase. The resulting suspensions were incubated on ice for 3 h and subjected to centrifugation at 149 000*g* in a Beckman airfuge for 10 min. The supernatant was carefully collected ($\sim$40 μL), and glycerol was added to a final concentration of 15% to facilitate sample application. To separate the enzyme complexes, a minigel format (Bio-Rad) with a 7% separating gel and a 4% stacking gel was employed here. Shortly before conducting the BN-PAGE, 8 μL of 5% Coomassie blue in 500 mM aminocaproic acid was added to the samples. Ten microliters of the above samples was then loaded into each well, and the BN-PAGE was performed in the cold room at 80 V until the protein samples entered into the stacking gel. The cathode buffer containing 0.02% Serva Blue G was then replaced by the same buffer but with only 0.002% dye. The electrophoresis was resumed and continued for 3 h at 200 V. At the end of electrophoresis, the gel was washed several times in 2 mM Tris-HCl (pH 7.5) buffer and then subjected to Western blotting followed by immunodetection using the affinity-purified anti-NuoB antibody.

Activity Assays. In contrast to mammalian mitochondria which contain complex I as the only NADH-quinone oxidoreductase, it is generally recognized that *E. coli* produces another type of NADH dehydrogenase, NDH-2. However, these two enzymes can be differentiated because only complex I/NDH-1 can use dNADH as a substrate (*33*). Therefore, dNADH was used as the respiratory substrate throughout the entire study. Enzymatic assays, which included dNADH oxidase activity, dNADH-DB reductase activity, and dNADH-$K_3Fe(CN)_6$ reductase activity, were conducted at 37 °C using a SLM DW-2000 spectrophotometer as described previously (*34*). For each measurement, *E. coli* membranes equivalent to 80 μg of protein per mL of assay mixture were used. To test the capsaicin sensitivity of the NDH-1, 10 μM of a synthetic analogue (cap-40) was used to inhibit the reaction (*35*). For DCCD inhibition tests, the *E. coli* membranes (10 μg/μL) were first treated with 2 mM DCCD for 4 h at room temperature and assayed for dNADH-DB reductase activity. Equal volume of ethanol (the solvent used to dissolve DCCD) was added to the membrane samples as a control. The initial activities were calculated by using extinction coefficients of 6.22 mM^{-1} cm^{-1} for dNADH and 1.00 mM^{-1} cm^{-1} for $K_3Fe(CN)_6$. Membrane potential (inside positive) and proton gradient (inside acidic) were measured using inside-out *E. coli* membrane vesicles as reported previously (*26*). Briefly, membrane potential was monitored using oxonol VI by recording absorbance change at 630 $-$ 603 nm. Formation of proton gradient was observed by following fluorescence quenching of ACMA, as described by Amarneh and Vik (*36*). The respiratory substrate was 0.2 mM dNADH. Uncoupler FCCP, potassium ionophore valinomycin, and electroneutral K^+/H^+ exchanger nigericin were added as indicated.

Other Analytical Procedures. Protein concentrations were determined by the BCA protein assay kit (Pierce) using bovine serum albumin as the standard according to the manufacturer's instruction. Any variations from the procedures and other details are described in the figure legends.

RESULTS

Sequence Analysis of the NuoK Subunit. Figure 2A shows the amino acid sequence alignment of subunit NuoK/Nqo11/ND4L from diverse sources ranging from mammals to bacteria. When compared to other subunits of NDH-1/complex I, NuoK is one of the less-conserved subunits. The *E. coli* NuoK subunit and the human ND4L subunit share only 23% sequence similarity. Despite the significant difference in the primary structure, the hydropathy profiles of these homologous NuoK/Nqo11/ND4L subunits are actually quite similar. Figure 2B presents a hypothetical topology of the *E. coli* NuoK subunit which was drawn based on the experimentally determined topology of the *P. denitrificans* Nqo11 (NuoK) subunit (*15*) together with the predictions obtained from several well-adopted computer programs such as TMHMM (*37*), TopPred2 (*38*), TMpred (*39*), and HMMTOP (*40*). The *E. coli* NuoK subunit is predicted to contain three transmembrane segments (designated TM1$-$3 from N- to C-terminus), with the N- and the C-terminal region oriented toward the periplasmic and the cytoplasmic side of the membrane, respectively. According to the sequence alignment, only seven residues are well-conserved in this subunit. Among them, two highly conserved glutamates, Glu-36 and Glu-72 (*E. coli* numbering), are of particular interest because they are predicted to be deeply embedded in TM2 and TM3, respectively, and have a functional group capable of participating in proton translocation. Our database search revealed that Glu-36 is almost perfectly conserved among all species and Glu-72 is highly conserved except that, in some parasites, this residue is replaced by serine. Another highly conserved residue, Arg-25, which is predicted to reside in a short loop connecting TM1 and TM2, also carries a charged group. As for Arg-85 and Arg-87, they are well-conserved in bacteria but not in eukaryotes. These two residues are close to the C-terminal end which is located in the cytoplasm.

On the basis of the above sequence analyses, we first constructed 10 site-specific NuoK mutants including the two conserved Glu residues in the transmembrane segments and the three Arg residues located on the cytosolic side (R25A, R25K, E36A, E36Q, E72A, E72Q, R85A, R85K, R87A, and R87K). In the second set of mutations, we targeted two highly conserved residues in the TM1 and an additional Arg residue in a cytosolic loop (F15A, G21V, R26A, R26K, and R25A/R26A). The correct generation of these mutations was confirmed by DNA sequencing.

Effects of NuoK Mutation on the NDH-1 Activity. In addition to NDH-1, *E. coli* also contains another NADH-quinone oxidoreductase, NDH-2. The *E. coli* NDH-2 is a small, FAD-dependent enzyme which is not sensitive to capsaicin and cannot use dNADH as a substrate (*33*). It does not couple electron transport to proton translocation. In our preliminary studies, NADH-driven respiration of the wild-type membranes was 65% sensitive to capsaicin, indicating that $\sim$35% of the NADH oxidase activity was ascribed to NDH-2 (data not shown). To measure the activities derived solely form NDH-1, we used dNADH as the substrate. We conducted three types of assays, namely, dNADH oxidase

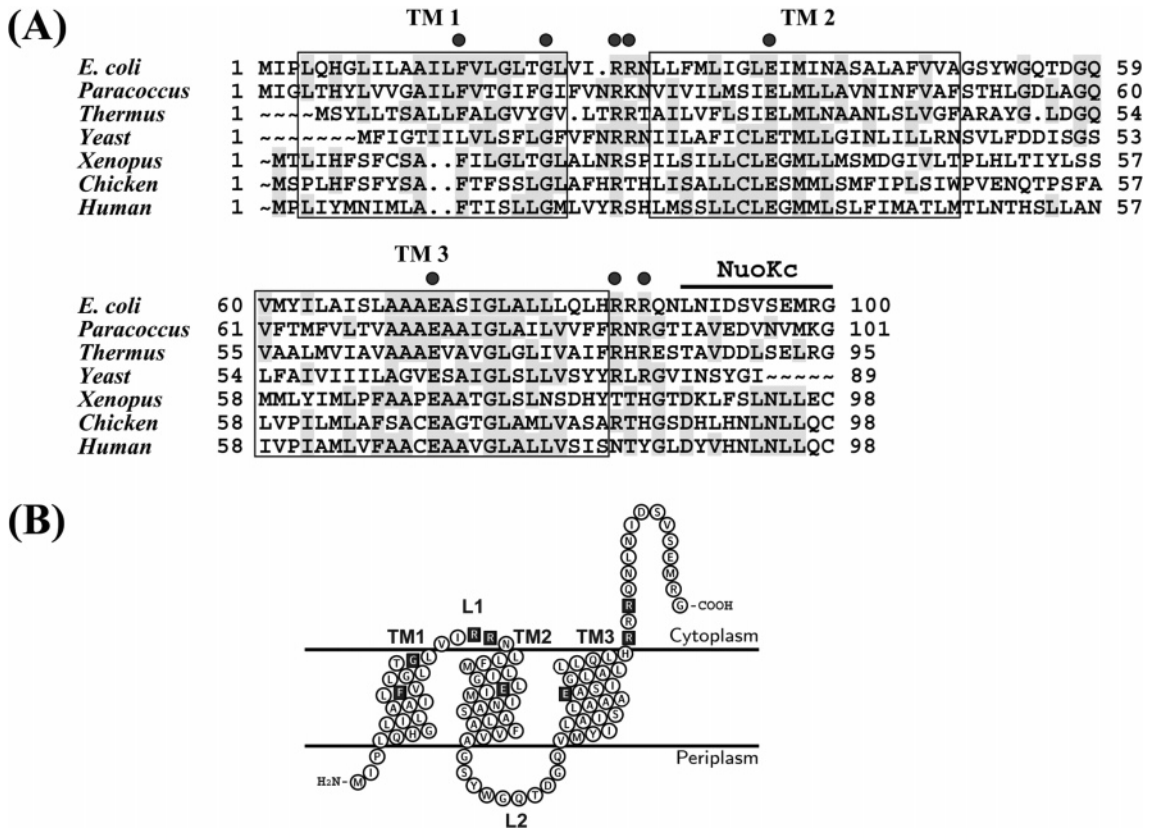

FIGURE 2: (A) Comparison of the deduced amino acid sequence of the *E. coli* NuoK subunit with its homologues from various organisms. The alignment was carried out by using the PILEUP programs of GCG software (*42*). Sequence sources and their Swiss-Prot accession numbers are (from top to bottom) *E. coli* K-12 [P33606], *P. denitrificans* [P29923], *Thermus thermophilus* HB-8 [Q56226], yeast *Yarrowia lipolytica* [Q9B6D4], *Xenopus laevis* [P03904], chicken *Gallus gallus* [P18942], and *Homo sapiens* [P03901]. Amino acid residues mutated in this study are marked by dots. Three predicted transmembrane segments (TM1−3) are enclosed in boxes (see Figure 2B for details). The segment marked NuoKc indicates the oligopeptide region used to raise the antibody specific to the C-terminal region of the *E. coli* NuoK. (B) Proposed topology of the *E. coli* NuoK subunit. The prediction has been performed on the basis of the reported topology of its *Paracoccus* counterpart (*15*). As described in Results, the three transmembrane segments of the *E. coli* NuoK subunit from the N-terminus to the C-terminus are designated TM1−3. The loops are designated L1 and L2. The N-terminus and C-terminus of the subunit are exposed to the periplasmic side and the cytoplasmic side of the membrane, respectively. The mutated amino acid residues are displayed by black squares.

activity, dNADH-DB reductase activity, and dNADH dehydrogenase activity, to assess the effects of the mutations.

Because the point mutants were checked only by sequencing the *nuoK* gene and its flanking regions, we could not rule out a possibility that introduction of any modification during the gene replacement process altered other essential genes. To address this question, we reintroduced the native *nuoK* gene into the knock-out mutant by following the same procedure used to generate point mutants (KO-rev mutant). As shown in Table 2, the KO-rev mutant displayed properties indistinguishable from the wild-type strain in all enzymatic activities tested. This proved that the procedure used to introduce point mutations in the chromosome did not have any modification at the protein level that affected the NDH-1 respiratory function. Consequently, the KO-rev mutant could serve as an appropriate reference strain in addition to the original MC4100 wild-type strain.

The point mutants constructed displayed different degrees of inhibition of dNADH oxidase activity and dNADH-DB reductase activity. We note that the two activities behaved in a similar manner among the mutants tested, implying that the observed effects are due mainly to the NDH-1 mutations but not to alteration of the downstream enzymes. Mutation of the highly conserved Glu residues in the transmembrane segments (E36 and E72) had the greatest impact, almost total abolishment of activities with E36A and E36Q and significantly reduced activities with E72A and E72Q. These results agree with those reported by Kervinen et al. (*25*), in which mutants E36Q and E72Q were shown to have the phenotype of poor growth on malate. Among the three Arg residues tested, mutation of Arg-25, which is located in a loop connecting TM1 and TM2, resulted in ∼70% reduction (R25A and R25K) in the activities, while mutation of the other two did not have any appreciable effects. This prompted us to investigate Arg-26 that is adjacent to Arg-25 in the same cytosolic loop. Unlike the Arg-25 mutation, placing a Lys (R26K) residue did not cause the activity reduction. However, the Ala substitute (R26A) gave rise to 64% inhibition, almost to the same extent as that in the R25 mutants. These residual activities were further lowered when both Arg-25 and Arg-26 were replaced with Ala in a double mutant (R25A/R26A). In the second set of experiment, we have included two residues, F15 and G21, both of which are located in the TM1 and are highly conserved among species. The activity decrease was either small (F15A) or moderate (G21V).

It is generally recognized that cap-40 acts as a competitive inhibitor for quinone in NDH-1/complex I and represses only energy-coupled activities (*35*) and that the binding site of this inhibitor is located within the membrane domain of the

Table 2: Enzyme Activities of the Membrane-Bound NDH-1 of *E. coli* Wild-Type and Various NuoK Mutants

	NDH-1 activities[a]				
	dNADH−O_2		dNADH-DB		dNADH−$K_3Fe(CN)_6$
NuoK mutant	(nmol dNADH/mg protein) /min	I_{50} (Cap-40)[b]	(nmol dNADH/mg protein) /min	DCCD inhibition[c]	(nmol $K_3Fe(CN)_6$/mg protein) /min
wild	469 ± 20 (100%)	0.13	571 ± 24 (100%)	71%	1278 ± 27 (100%)
KO	5 ± 1 (1%)		39 ± 4 (7%)		180 ± 5 (14%)
KO-rev	466 ± 18 (99%)	0.11	566 ± 22 (99%)	72%	1297 ± 21 (101%)
R25A	121 ± 4 (26%)	0.10	151 ± 6 (26%)	67%	1246 ± 50 (97%)
R25K	132 ± 6 (28%)	0.10	176 ± 7 (31%)	71%	1252 ± 26 (98%)
E36A	6 ± 2 (1%)		40 ± 4 (7%)		1211 ± 34 (95%)
E36Q	12 ± 2 (3%)		42 ± 4 (7%)		1270 ± 29 (99%)
E72A	201 ± 9 (43%)	0.12	273 ± 12 (48%)	67%	1316 ± 27 (103%)
E72Q	108 ± 5 (22%)	0.10	149 ± 5 (26%)	69%	1269 ± 26 (99%)
R85A	469 ± 21 (100%)	0.14	564 ± 25 (99%)	70%	1332 ± 38 (104%)
R85K	458 ± 16 (98%)	0.14	556 ± 11 (97%)	71%	1312 ± 29 (103%)
R87A	460 ± 16 (98%)	0.13	568 ± 13 (99%)	70%	1321 ± 25 (103%)
R87K	512 ± 17 (107%)	0.14	603 ± 25 (106%)	73%	1355 ± 24 (106%)
F15A	412 ± 18 (88%)	0.14	514 ± 18 (90%)	72%	1306 ± 17 (102%)
G21V	273 ± 10 (58%)	0.10	351 ± 8 (61%)	70%	1268 ± 23 (99%)
R26A	171 ± 6 (36%)	0.09	222 ± 9 (39%)	65%	1158 ± 18 (91%)
R26K	483 ± 20 (103%)	0.14	620 ± 14 (109%)	77%	1227 ± 23 (96%)
R25A/R26A	66 ± 3 (14%)		80 ± 4 (14%)		1150 ± 20 (90%)

[a] Activities were measured at least three times and given as the mean ± standard deviation. The assays were conducted at 37 °C. [b] The concentration of capsaicin-40 (μM) that causes 50% inhibition. [c] Percent inhibition of the dNADH-DB activity after DCCD treatment at 2 mM for 4 h at room temperature.

complex. In our preparation of *E. coli* membranes from the wild-type strain, the dNADH-dependent respiration was inhibitable up to 97% by cap-40 (data not shown). We then investigated the inhibition effects using the NuoK mutants constructed. As shown in Table 2, no significant difference in the I_{50} values of cap-40 between wild-type and the mutants was found, suggesting that the cap-40 binding site is not modified by these point mutations. However, involvement of Glu-36 in cap-40 binding remains to be seen because the activity was too low to be analyzed.

Another inhibitor that acts upon the membrane domain and specifically diminishes the energy-coupled activity of NDH-1/complex I is DCCD. Therefore, we surveyed the mutants for their sensitivity to DCCD. In this case the dNADH-DB activity was measured because of possible inhibition of terminal oxidase by DCCD. All point mutants examined showed the same degree of DCCD inhibition as the wild-type strain. Again, activities of the Glu-36 mutants were too low to yield reliable data.

Table 2 includes dNADH-$K_3Fe(CN)_6$ reductase activity of all mutants together with wild-type. This activity derives from the NADH dehydrogenase segment of the complex I /NDH-1 and, therefore, could be used as an estimate for the amount of active peripheral domain associated with the membrane. The knock-out mutant retained only 14% of dNADH-$K_3Fe(CN)_6$ reductase activity as compared to wild-type membranes, indicating that most of the functionally active peripheral arm was absent when the enzyme was devoid of the NuoK subunit. We have observed similar results with NuoA (*29*) and NuoJ (*26*) knock-out mutants. In contrast, all constructed point mutants invariantly exhibited the same activity as wild-type. Therefore, it seems likely that none of the point mutations introduced in the NuoK subunit caused loss of the peripheral domain. However, a precise assessment of the assembly status requires more direct methods such as determination of the subunit contents of the individual membrane preparations as described below.

Subunit Contents of NDH-1 of NuoK Mutants. Immunochemical analyses were performed to systematically examine the subunit contents of the NDH-1 in the cytoplasmic membranes from all NuoK mutants. We selected a total of nine subunit-specific antibodies for detection; three antibodies are against subunits present in the membrane domain (NuoK, NuoJ, and NuoA) and six antibodies against subunits located in the peripheral domain (NuoB, NuoCD, NuoE, NuoF, NuoG, and NuoI) (Figure 3). In our preliminary studies, antibodies against NuoKc, NuoJc, NuoAc, NuoCD, NuoE, NuoF, NuoG, NuoB, and NuoI recognized a band in the *E. coli* membranes with an apparent molecular mass of 11-, 21-, 16-, 65-, 20-, 50-, 91-, 22-, and 21-kDa, respectively.

As shown in Figure 3, the antibody specific to NuoKc reacted with wild-type but did not react with the NuoK knock-out mutant. In addition, the same antibody also recognized a band in all point mutants with signal intensities similar to those of the wild-type membranes, indicating that the NuoK subunit was expressed and assembled in the membranes of all NuoK point mutants. It is worthwhile mentioning that the NuoK subunit of E72A exhibited slightly slower electrophoretic mobility as compared to the wild-type strain. We have observed similar mobility abnormality for the *E. coli* NuoA subunit mutant D79A (*29*). In that case, the abnormal mobility of the NuoA subunit was improved significantly by suspending the membranes in the Laemmli's sample buffer with an additional 4 M urea, followed by incubation in the boiling water for 10 min before loading on the SDS gels. However, when the same harsh conditions were applied to the sample treatment in this study, the NuoK subunit aggregated and did not enter the gel (data not shown). As for the other membrane domain subunits tested, NuoA and NuoJ were also missing from the membranes of the NuoK knock-out mutant. Interestingly, divergent results were observed in the subunits that made up the peripheral domain of the *E. coli* NDH-1. As seen in Figure 3, small amounts

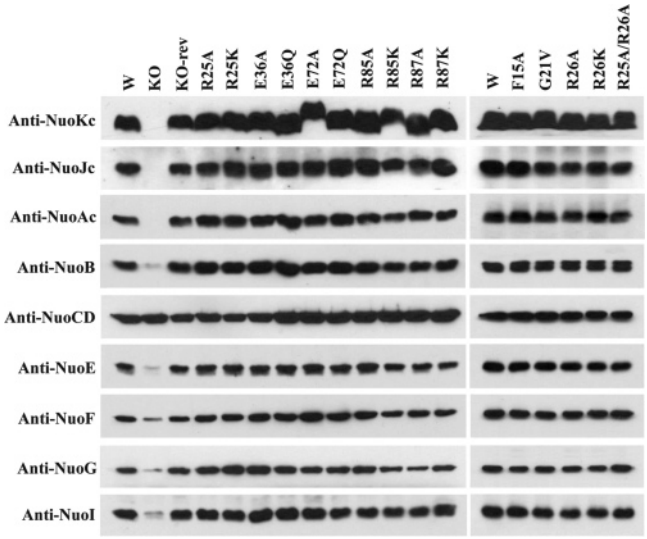

FIGURE 3: Immunoblotting of membrane preparations from the wild-type (W), NuoK knock-out (KO), NuoK revertant (KO-rev), and site-specific NuoK mutants. Antibodies specific to NuoKc, NuoJc, NuoAc, NuoB, NuoCD, NuoE, NuoF, NuoG, and NuoI were used. *E. coli* membranes (10 μg of protein per lane) were loaded on a 13% Laemmli SDS polyacrylamide gel. After electrophoresis, the proteins were transferred to nitrocellulose membranes and Western blotting was carried out with SuperSignal West Pico system (Pierce) according to Han et al. (*30*). The secondary antibody used for detection was goat anti-rabbit IgG horseradish peroxidase conjugate (Pierce).

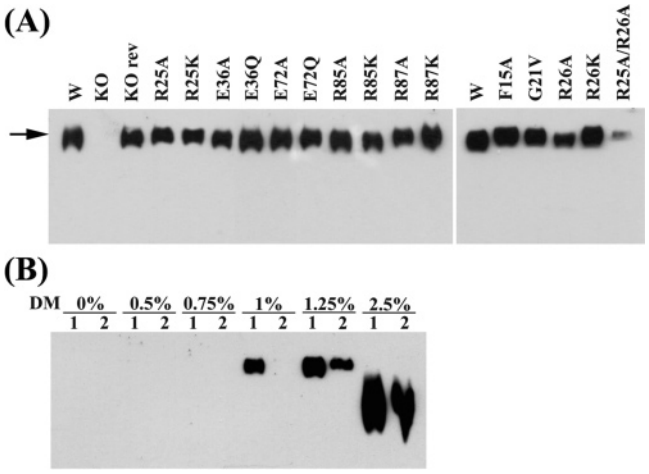

FIGURE 4: Immunoblotting of BN-PAGE gels of membrane preparations from *E. coli*. The electrophoresis was performed as described in Experimental Procedures. After BN-PAGE, the *E. coli* membrane proteins were transferred to nitrocellulose membranes. Subsequently, the nitrocellulose membranes were immunostained with the affinity-purified NuoB antibody as described in Figure 3. (A) Membranes from the wild-type (W), NuoK knock-out (KO), NuoK revertant (KO-rev), and NuoK point mutants were compared. The dodecyl maltoside concentration was 1.25%. The arrow shows the location of the band recognized by the anti-NuoB antibody. (B) Membranes from the wild-type (1) and the R25A/R26A double mutant (2) were solubilized at the indicated concentrations of dodecyl maltoside (DM). Other conditions were the same as in panel A.

of NuoB, NuoE, NuoF, NuoG, and NuoI subunits were present in the membranes of NuoK knock-out cells, whereas the amounts of the NuoCD subunit appeared to be the same as those found in the membranes of the wild-type strain. This observation may seem to indicate that NuoK is required for efficient assembly of the NDH-1 complex. However, the exact role of the NuoK subunit on the assembly of NDH-1 must be evaluated when antibodies against other membrane domain subunits (i.e., NuoH, NuoN, NuoM, and NuoL) become available. As for the NuoK point mutants, the intensities of signals corresponding to all the tested subunits in the membranes were comparable to those found in the wild-type membranes. Apparently, none of the mutations generated in this study had any appreciable change in the subunit contents of NDH-1.

Subunit Assembly of NDH-1 of NuoK Mutants. To directly verify the presence of assembled NDH-1 in the constructed mutants, we used BN-PAGE to analyze these membrane samples. After BN-PAGE, the amount of the fully assembled complex was evaluated through immunoblotting using an antibody specific to the NuoB subunit. As illustrated in Figure 4A, no intact NDH-1 was observed in the NuoK knock-out mutant. In contrast, membranes isolated from the wild-type and all site-specific NuoK mutants, except for the double mutant R25A/R26A, seemed to contain similar amounts of fully assembled NDH-1. The results are mostly in good agreement with the data obtained from the assay of dNADH-$K_3Fe(CN)_6$ reductase activity. The R25A/R26A mutant, however, displayed a greatly diminished level of the assembled complex despite the fact that it has full dNADH-$K_3Fe(CN)_6$ activity. We suspected that the discrepancy might be due to a procedural difference between the activity measurement and the BN-PAGE. Because the BN-PAGE requires dissociation of the membrane using dodecyl maltoside, we ran the experiment with increasing concentrations of this detergent and compared the results between wild-type and the R25A/R26A mutant. The result is shown in Figure 4B. At 1% dodecyl maltoside, the NDH-1 is visible only in wild-type. When the detergent concentration was increased to 1.25%, which is our regular condition, the mutant showed the NDH-1 band but the signal was less than the wild-type sample. At a higher detergent concentration, the density of the band increased for both wild-type and the mutant and the migration pattern was now skewed. Evidently, the NDH-1 complex of the R25A/R26A mutant is more resistant to the detergent and thus tends to show decreased intensity on the BN-PAGE unless an excess amount of detergent is employed. It is conceivable from the results of contents of the individual subunits and the whole enzyme complex that none of the site-specific NuoK mutations introduced in this study affected the assembly of NDH-1 complex.

Measurements of Electrochemical Potential of NuoK Mutants. Since electron transfer activities of the mutants varied from normal to almost null without any effects on the assembly of the enzyme, it was of interest to examine the generation of membrane potential and proton gradient. Membrane potential was monitored by following the absorbance change of a reporter dye, oxonol VI. Figure 5 shows representative traces of oxonol response. Addition of dNADH to the membrane vesicles prepared from the wild-type strain increased the signal indicating the generation of $\Delta\Psi$ (inside positive) which was then dissipated by an uncoupler, FCCP. The signal was enhanced in the presence of nigericin and totally abolished by nigericin and valinomycin as expected (data not shown). Preincubation of the membrane samples with an inhibitory concentration of cap-40 also prevented the $\Delta\Psi$ formation (data not shown). As anticipated, no $\Delta\Psi$

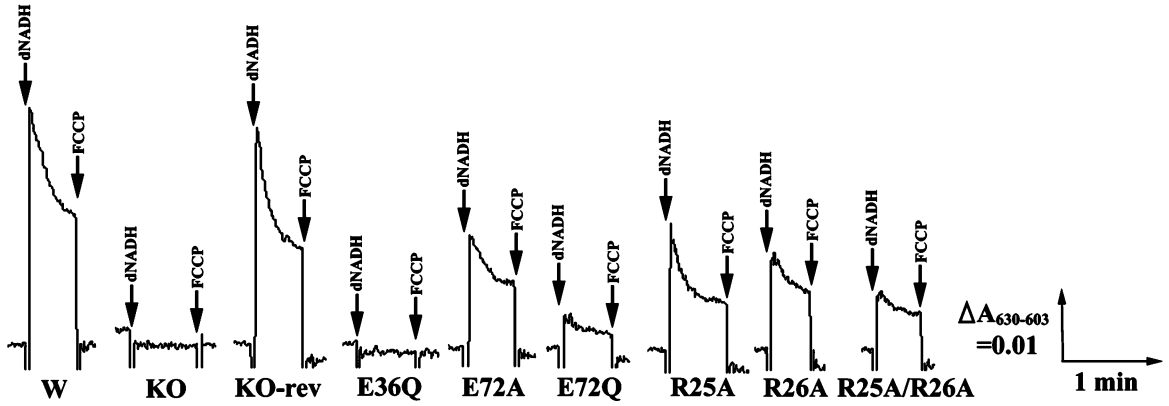

FIGURE 5: Detection of the membrane potential generated by dNADH oxidation in *E. coli* NuoK mutants. Membranes were prepared from each of the constructed mutants, and the membrane potential was monitored by the absorbance change of oxonol VI at 630 − 603 nm at 37 °C. At the time indicated by arrows, 0.2 mM dNADH or 2 μM FCCP was added to an assay mixture containing 50 mM MOPS (pH7.3), 10 mM $MgCl_2$, 50 mM KCl, 2 μM oxonol VI, and *E. coli* membrane samples (400 μg of protein/mL).

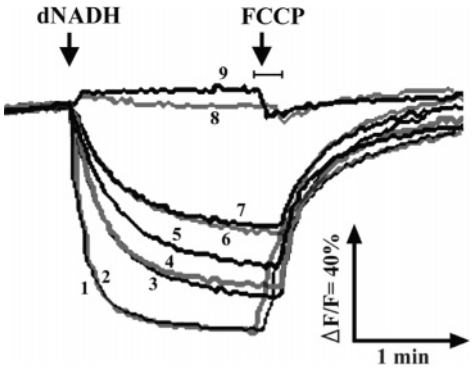

FIGURE 6: Generation of a pH gradient by dNADH oxidation in *E. coli* NuoK mutants. Membranes were prepared from each of the constructed mutants, and the extent of proton translocation was measured by the quenching of the fluorescence of ACMA at room temperature with an excitation wavelength of 410 nm and an emission wavelength of 480 nm. At the time indicated by arrows, 0.2 mM dNADH or 10 μM FCCP was added to an assay mixture containing 50 mM MOPS (pH7.3), 10 mM $MgCl_2$, 50 mM KCl, 2 μM ACMA, and *E. coli* membrane samples (150 μg of protein/mL). Traces are 1, wild-type; 2, NuoK revertant; 3, R26A; 4, R25A; 5, E72A; 6, R25A/R26A; 7, E72Q; 8, E36Q; and 9, knock-out.

was observed in the membranes of the knock-out mutant, and the membrane vesicles of KO-rev mutant generated a signal comparable to that of the wild-type strain. Mutation of highly conserved Glu-36, to either Ala or Glu, resulted in a complete loss of the ability of the enzyme to generate $\Delta\Psi$. In the case of another highly conserved, acidic residue Glu-72, replacing the carboxyl group with an amide group caused a significant reduction in $\Delta\Psi$, whereas substituting Ala had a moderate effect. The same moderate diminution of $\Delta\Psi$ was seen with all mutants of Arg-25 and Arg-26. The double mutant R25A/R26A generated a $\Delta\Psi$ that is slightly less than that of R25A or R26A. Other mutants involving Arg-85, Arg-87, Phe-15, and Gly-21 all had a $\Delta\Psi$ somewhat smaller than that of the wild-type strain. When DB was used as the electron acceptor, basically the same results were obtained (data not shown).

The formation of proton gradient (ΔpH, inside acidic) was monitored through fluorescence quenching of ACMA. Representative traces are shown in Figure 6. Membrane vesicles from wild-type and the KO-rev mutant exhibited an almost identical response with a maximum quenching of 77% after addition of dNADH. The signal was then completely reversed by the addition of FCCP. No proton translocation activity was observed in the NuoK knock-out mutant. Similarly, the Glu-36 mutants did not show any sign of proton pumping activity. Membranes from E72Q and R25A/R26A had significantly lower fluorescence quenching (41−43%), whereas those from E72A, R25A, R25 K, R26A, and R26K exhibited moderate fluorescence quenching (56−67%). As for R85A, R85K, R87A, and R87K, they all displayed wild-type-like fluorescence quenching. Similar results were obtained using DB as the electron acceptor (data not shown). When compared, the data on ΔpH largely agreed with the data on $\Delta\Psi$.

DISCUSSION

Among the seven mtDNA-encoded subunits of complex I, the ND4L is the smallest subunit with only about 100 amino acid residues. The protein appears to have three putative transmembrane helices. Two highly conserved carboxyl residues, Glu-36 and Glu-72, of the *E. coli* NDH-1 are predicted to be located in the middle of the membrane. Recently, Kervinen et al. (*25*) reported that both carboxyl residues in *E. coli* were important for cell growth and enzyme activity. They adopted the in trans complementation approach in which the knock-out *nuoK* gene was complemented by an expression plasmid carrying a point-mutated *nuoK* gene. In this method, complementation with the normal *nuoK* gene yielded only partial restoration of the activity (about 10−20% in minimal medium and 40−50% in rich medium). Similar techniques used for complementation of the *R. capsulatus* NuoK knock-out mutant only restored 59% of the wild-type activity (*22*). One possible reason for the lack of full restoration is the polar effect that might influence the expression of the downstream genes. In the present study, we used homologous recombination to introduce site-directed mutations directly into the *E. coli* chromosome. With this approach, the KO-rev mutant constructed from the knockout mutant and the unmutated *nuoK* gene fully restored the NDH-1 function. Thus, this method ensures that the altered properties observed in the point mutants result solely from the mutations *per se* and not from possible artifacts. Our data indicated that mutations of Glu-36 completely abolished the coupled electron-transfer activities as well as formation of electrochemical gradient. Mutations of Glu-72 also exerted severe effects, although to a lesser extent. These results

confirm that the carboxyl groups at these particular locations in the NuoK subunit are important for normal NDH-1 functions.

A severe loss of enzymatic activities after mutating residue(s) of a subunit could possibly be due to a drastic alteration of the structure, such as incomplete assembly of the complex. However, our present study shows that this is not the case with our NuoK mutations. The NDH-1 of the mutants with the least activity still retained the same subunit contents as the wild-type strain as judged from Western blotting. Furthermore, the presence of the whole complex was confirmed by BN-PAGE across all the mutants. The combined results are far more convincing than the commonly used procedure of assessing the enzyme content with $K_3Fe(CN)_6$ reduction.

Recently, we have reported that simultaneous introduction of mutations in two carboxyl residues, Asp-79 and Glu-81, located in the middle of TM2 of the *E. coli* NuoA subunit (ND3 of complex I) almost totally abolished the energy-coupled activities (*29*). In addition, the replacement of a conserved valine with a glycine in the TM3 of the *E. coli* NuoJ subunit (ND6 of complex I) not only greatly reduced its NDH-1 activities but also caused a nearly complete loss of proton translocation (*26*). These results led us to suggest that a multihelix bundle contributed from more than one subunit may provide a structural and environmental basis for the proton translocation. The current study may add, to this bundle, the two Glu residues of the NuoK subunit that are shown to possibly participate, directly or indirectly, in the coupling mechanism. Despite the lack of information about the subunit arrangement of the NDH-1, a multihelix bundle proton channel consisting of the above three subunits is an attractive model because it reasonably integrates all the available data provided in this study and the previous results on NuoA and NuoJ.

Among the Arg residues predicted to be on the cytosolic side, those that are near the C-terminus do not seem to be critical for the function or structure of NDH-1. However, the Arg residues that are found on a small loop between TM1 and TM2 may have some active roles. The *E. coli* enzyme has two Arg residues in this region. One (Arg-25) is highly conserved, and the other (Arg-26) is not well-conserved. Mutating Arg-25, even conservatively to Lys, caused a significant reduction in the NDH-1 activities. More interestingly, replacing both Arg residues (R25A/R26A) had a drastic effect. In terms of activities, the double mutant resembled the E72Q mutant with greatly reduced electron-transfer rates and diminished electrochemical gradient. What was unexpected is that the NDH-1 complex with the double mutation was more resistant to detergent as revealed by the BN-PAGE experiment. It may be speculated that removal of Arg residue(s), but probably not by simple elimination of positive charges, may alter the way the cytosolic loop interacts with certain subunits in the peripheral domain. We can further envision that the altered interaction renders the whole complex rigid, and thereby, hampers dynamic movements presumed to be of importance for the indirect coupling mechanism (*1*). In slightly different but related consequences, Yadava et al. reported the presence of an essential Arg residue in the MWFE subunit of complex I (*41*). In this small membrane-associated subunit, a point mutation that led to a replacement of a highly conserved Arg to a Lys caused a complete loss of the enzyme activity, apparently due to lack of fully assembled complex I.

In this study we have conducted site-directed mutations by directly introducing mutations at the level of chromosomal DNA to explore functional and structural roles of the *E. coli* NuoK subunit in NDH-1. Together with the earlier application of this promising approach on subunits NuoA and NuoJ, it is clear that we can extend the study carried out on the bacterial system and gain a comprehensive view on complex I.

ACKNOWLEDGMENT

We thank Dr. Marta Perego (The Scripps Research Institute) for her help with chromosomal DNA manipulation and Drs. Byoung Boo Seo and Tetsuo Yamashita for stimulating discussion.

REFERENCES

1. Yagi, T., and Matsuno-Yagi, A. (2003) The proton-translocating NADH-quinone oxidoreductase in the respiratory chain: the secret unlocked, *Biochemistry 42*, 2266−2274.
2. Galkin, A. S., Grivennikova, V. G., and Vinogradov, A. D. (1999) →H^+/2e− stoichiometry in NADH-quinone reductase reactions catalyzed by bovine heart submitochondrial particles, *FEBS Lett. 451*, 157−161.
3. Carroll, J., Shannon, R. J., Fearnley, I. M., Walker, J. E., and Hirst, J. (2002) Definition of the nuclear encoded protein composition of bovine heart mitochondrial complex I: identification of two new subunits, *J. Biol. Chem. 277*, 50311−50317.
4. Friedrich, T., Abelmann, A., Brors, B., Guénebaut, V., Kintscher, L., Leonard, K., Rasmussen, T., Scheide, D., Schlitt, A., Schulte, U., and Weiss, H. (1998) Redox components and structure of the respiratory NADH:ubiquinone oxidoreductase (complex I), *Biochim. Biophys. Acta 1365*, 215−219.
5. Yagi, T., Yano, T., Di Bernardo, S., and Matsuno-Yagi, A. (1998) Procaryotic complex I (NDH-1), an overview, *Biochim. Biophys. Acta 1364*, 125−133.
6. Carroll, J., Fearnley, I. M., Shannon, R. J., Hirst, J., and Walker, J. E. (2003) Analysis of the subunit composition of complex I from bovine heart mitochondria, *Mol. Cell. Proteomics 2*, 117−126.
7. Guénebaut, V., Schlitt, A., Weiss, H., Leonard, K., and Friedrich, T. (1998) Consistent structure between bacterial and mitochondrial NADH:ubiquinone oxidoreductase (complex I), *J. Mol. Biol. 276*, 105−112.
8. Friedrich, T. (1998) The NADH:ubiquinone oxidoreductase (complex I) from *Escherichia coli*, *Biochim. Biophys. Acta 1364*, 134−146.
9. Takano, S., Yano, T., and Yagi, T. (1996) Structural studies of the proton-translocating NADH-quinone oxidoreductase (NDH-1) of *Paracoccus denitrificans*: identity, property, and stoichiometry of the peripheral subunits, *Biochemistry 35*, 9120−9127.
10. Yano, T., and Yagi, T. (1999) H^+-translocating NADH-quinone oxidoreductase (NDH-1) of *Paracoccus denitrificans*: studies on topology and stoichiometry of the peripheral subunits, *J. Biol. Chem. 274*, 28606−28611.
11. Di Bernardo, S., and Yagi, T. (2001) Direct interaction between a membrane domain subunit and a connector subunit in the H^+-translocating NADH-quinone oxidoreductase, *FEBS Lett. 508*, 385−388.
12. Kao, M.-C., Matsuno-Yagi, A., and Yagi, T. (2004) Subunit proximity in the H^+-translocating NADH-quinone oxidoreductase probed by zero-length cross-linking, *Biochemistry 43*, 3750−3755.
13. Yano, T., Magnitsky, S., Sled', V. D., Ohnishi, T., and Yagi, T. (1999) Characterization of the putative 2x[4Fe-4S] binding NQO9 subunit of the proton-translocating NADH-quinone oxidoreductase (NDH-1) of *Paracoccus denitrificans*: expression, reconstitution, and EPR characterization, *J. Biol. Chem. 274*, 28598−28605.
14. Di Bernardo, S., Yano, T., and Yagi, T. (2000) Exploring the membrane domain of the reduced nicotinamide adenine dinucleotide-quinone oxidoreductase of *Paracoccus denitrificans*: characterization of the NQO7 subunit, *Biochemistry 39*, 9411−9418.

15. Kao, M.-C., Di Bernardo, S., Matsuno-Yagi, A., and Yagi, T. (2002) Characterization of the membrane domain Nqo11 subunit of the proton-translocating NADH-quinone oxidoreductase of *Paracoccus* denitrificans, *Biochemistry 41*, 4377−4384.
16. Kao, M.-C., Di Bernardo, S., Matsuno-Yagi, A., and Yagi, T. (2003) Characterization and topology of the membrane domain Nqo10 subunit of the proton-translocating NADH-quinone oxidoreductase of *Paracoccus denitrificans*, *Biochemistry 42*, 4534−4543.
17. Chomyn, A., Mariottini, P., Cleeter, M. W. J., Ragan, C. I., Matsuno-Yagi, A., Hatefi, Y., Doolittle, R. F., and Attardi, G. (1985) Six unidentified reading frames of human mitochondrial DNA encode components of the respiratory-chain NADH dehydrogenase, *Nature 314*, 591−597.
18. Chomyn, A., Cleeter, M. W. J., Ragan, C. I., Riley, M., Doolittle, R. F., and Attardi, G. (1986) URF6, last unidentified reading frame of human mtDNA, codes for an NADH dehydrogenase subunit, *Science 234*, 614−618.
19. Nakamaru-Ogiso, E., Sakamoto, K., Matsuno-Yagi, A., Miyoshi, H., and Yagi, T. (2003) The ND5 subunit was labeled by a photoaffinity analogue of fenpyroximate in bovine mitochondrial complex I, *Biochemistry 42*, 746−754.
20. Gong, X., Xie, T., Yu, L., Hesterberg, M., Scheide, D., Friedrich, T., and Yu, C. A. (2003) The ubiquinone-binding site in NADH: ubiquinone oxidoreductase from *Escherichia coli*, *J. Biol. Chem. 278*, 25731−25737.
21. Steuber, J. (2003) The C-terminally truncated nuol subunit (ND5 homologue) of the Na^+-dependent complex I from *Escherichia coli* transports Na^+, *J. Biol. Chem. 278*, 26817−26822.
22. Dupuis, A., Darrouzet, E., Duborjal, H., Pierrard, B., Chevallet, M., Van Belzen, R., Albracht, S. P., and Lunardi, J. (1998) Distal genes of the *nuo* operon of *Rhodobacter capsulatus* equivalent to the mitochondrial ND subunits are all essential for the biogenesis of the respiratory NADH-ubiquinone oxidoreductase, *Mol. Microbiol. 28*, 531−541.
23. Finel, M. (1998) Organization and evolution of structural elements within complex I, *Biochim. Biophys. Acta 1364*, 112−121.
24. Mathiesen, C., and Hagerhall, C. (2003) The 'antiporter module' of respiratory chain complex I includes the MrpC/NuoK subunit—a revision of the modular evolution scheme, *FEBS Lett. 549*, 7−13.
25. Kervinen, M., Patsi, J., Finel, M., and Hassinen, I. E. (2004) A pair of membrane-embedded acidic residues in the NuoK subunit of *Escherichia coli* NDH-1, a counterpart of the ND4L subunit of the mitochondrial complex I, are required for high ubiquinone reductase activity, *Biochemistry 43*, 773−781.
26. Kao, M.-C., Di Bernardo, S., Nakamaru-Ogiso, E., Miyoshi, H., Matsuno-Yagi, A., and Yagi, T. (2005) Characterization of the membrane domain subunit NuoJ (ND6) of the NADH-quinone oxidoreductase from *Escherichia coli* by chromosomal DNA manipulation, *Biochemistry 44*, 3562−3571.
27. Murphy, E., Huwyler, L., and Freire Bastos, M. C. (1985) Transposon Tn554: complete nucleotide sequence and isolation of transposition-defective and antibiotic-sensitive mutants, *EMBO J. 4*, 3357−3365.
28. Link, A. J., Phillips, D., and Church, G. M. (1997) Methods for generating precise deletions and insertions in the genome of wild-type *Escherichia coli*: application to open reading frame characterization, *J. Bacteriol. 179*, 6228−6237.
29. Kao, M.-C., Di Bernardo, S., Perego, M., Nakamaru-Ogiso, E., Matsuno-Yagi, A., and Yagi, T. (2004) Functional roles of four conserved charged residues in the membrane domain subunit NuoA of the proton-translocating NADH-quinone oxidoreductase from *Escherichia coli*, *J. Biol. Chem. 279*, 32360−32366.
30. Han, A.-L., Yagi, T., and Hatefi, Y. (1989) Studies on the structure of NADH:ubiquinone oxidoreductase complex: topography of the subunits of the iron−sulfur protein component, *Arch. Biochem. Biophys. 275*, 166−173.
31. Laemmli, U. K. (1970) Cleavage of structural proteins during the assembly of the head of bacteriophage T4, *Nature 227*, 680−685.
32. Schagger, H., and Von Jagow, G. (1991) Blue native electrophoresis for isolation of membrane protein complexes in enzymatically active form, *Anal. Biochem. 199*, 223−231.
33. Matsushita, K., Ohnishi, T., and Kaback, H. R. (1987) NADH-ubiquinone oxidoreductases of the *Escherichia coli* aerobic respiratory chain, *Biochemistry 26*, 7732−7737.
34. Yagi, T. (1986) Purification and characterization of NADH dehydrogenase complex from *Paracoccus denitrificans*, *Arch. Biochem. Biophys. 250*, 302−311.
35. Satoh, T., Miyoshi, H., Sakamoto, K., and Iwamura, H. (1996) Comparison of the inhibitory action of synthetic capsaicin analogues with various NADH-ubiquinone oxidoreductases, *Biochim. Biophys. Acta 1273*, 21−30.
36. Amarneh, B., and Vik, S. B. (2003) Mutagenesis of subunit N of the *Escherichia coli* complex I. Identification of the initiation codon and the sensitivity of mutants to decylubiquinone, *Biochemistry 42*, 4800−4808.
37. Krogh, A., Larsson, B., Von Heijne, G., and Sonnhammer, E. L. L. (2001) Predicting trnasmembrane protein topology with a hidden Markov model: application to complete genomes, *J. Mol. Biol. 305*, 567−580.
38. Claros, M. G., and Von Heijne, G. (1994) TopPred II: an improved software for membrane protein structure predictions, *Comput. Appl. Biosci. 10*, 685−686.
39. Hofmann, K., and Stoffel, W. (1993) tmbase—a database of membrane spanning proteins segments, *Biol. Chem. Hoppe−Seyler 374*, 166.
40. Tusnády, G. E., and Simon, I. (2001) The HMMTOP transmembrane topology prediction server, *Bioinformatics 17*, 849−850.
41. Yadava, N., Potluri, P., Smith, E. N., Bisevac, A., and Scheffler, I. E. (2002) Species-specific and mutant MWFE proteins: their effect on the assembly of a functional mammalian mitochondrial complex I, *J. Biol. Chem. 277*, 21221−21230.
42. Devereux, J., Haeberli, P., and Smithies, O. (1984) A comprehensive set of sequence analysis programs for the VAX, *Nucleic Acids Res. 12*, 387−395.

BI050708W